Nonlinear superheat and capacity control of a refrigeration plant

Rasmussen, Henrik; Larsen, Lars F. S.

Published in:
17th Mediterranean Conference on Control and Automation

DOI (link to publication from Publisher):
10.1109/MED.2009.5164688

Publication date:
2009

Document Version
Publisher's PDF, also known as Version of record

Nonlinear superheat and capacity control of a refrigeration plant

Henrik Rasmussen
Department of Electronic Systems
Aalborg University
DK-9200 Aalborg, Denmark
Email: hr@es.aau.dk

Lars F. S. Larsen
Danfoss A/S, Nordborg, Denmark
Email: Lars.Larsen@Danfoss.com

***Abstract*—This paper proposes a novel method for superheat and capacity control of refrigeration systems. A new low order nonlinear model of the evaporator is developed and used in a backstepping design of a nonlinear controller. The stability of the proposed method is validated theoretically by Lyapunov analysis and experimental results shows the performance of the system for a wide range of operating points. The method is compared to a conventional method based on a thermostatic superheat controller.**

NOMENCLATURE

p	time derivative operator d/dt
L_e	length of the evaporator
l_e	length of the evaporator two phase section
$\dot{m}_e$	refrigerant mass flow rate
h_i	specific enthalpy, inlet evaporator
h_g	specific enthalpy, end of two phase section evaporator
h_o	specific enthalpy, outlet evaporator
h_{lg}	specific evaporation energy, refrigerant
T_e	refrigerant boiling temperature
P_e	refrigerant pressure, evaporator
f_c	compressor speed
T_{SH}	superheat, evaporator
$T_{w,in}$	temperature of water into the evaporator
$T_{w,out}$	temperature of water out of the evaporator
$\dot{m}_w$	mass flow of water
c_w	specific heat capacity of water
α_w	heat transfer coefficient water-wall
α_e	heat transfer coefficient refrigerant-wall
B	width of evaporator
H	hight of evaporator

I. INTRODUCTION

The basic components in a refrigeration system are expansion valve, evaporator, compressor and condenser. One of the key variables that greatly effects the efficiency of the system, is the filling of the evaporator. The filling is indirectly measured by the superheat defined as the difference between the outlet temperature of the gas and the evaporation temperature. Conventionally the superheat is controlled by adjusting the opening degree of the expansion valve. To utilize the potential of the evaporator to its maximum the filling should be as high as possible, i.e. the superheat should be kept as low as possible. This is a common control strategy and examples can be found in [8], [7] and [9]. However the fact that the superheat is highly nonlinear depended on the point of operation, the evaporator design and the characteristic of the expansion valve, limits the obtainable performance with standard PID controllers. Previously work by [4] and [6] has proved that gain scheduling

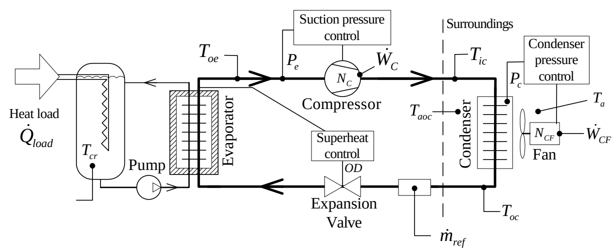

Fig. 1. Layout of the test refrigeration system including conventional control loops.

is a way to handle these gain variations. In a refrigeration system with variable speed compressor controlling the suction pressure and an expansion valve controlling the superheat the effect of cross coupling between the loops (hunting) may lead to instability or unacceptable performance, as described in [11]. Motivated by these difficulties, this paper proposes a novel approach to a model-based superheat and capacity control. As for the conventional controller the new control strategy controls the superheat temperature by the the opening degree of the expansion valve and the suction pressure by the compressor speed. Based on a develloped low order nonlinear model, with refrigerant flow and compressor speed as input and superheat temperature and suction pressure as output, a method based on backstepping is used for the controller design. Because backstepping design is based on Lyapunov stability, the controller is stable with a nerly perfect decoubling between capacity and superheat temperature for resonable coice of gains in the controller. Experiments on a test system shows an excellent performance both during startup and for variation of coling capacity by step change of the compressor speed between minimum and maximum. The new controller is also compared to a conventional controller based on a thermostatic expansion valve (TXV) for controlling of the superheat.

II. SYSTEM DESCRIPTION

The test system fig. 1 is a simple refrigeration system with water circulating through the evaporator. The heat load on the system is maintained by an electrical water heater with an adjustable power supply for the heating element. The compressor, the evaporator fan and the condenser pump are equipped with variable speed drives so that the rotational speed can be adjusted continuously. The system is furthermore equipped with an electronic expansion valve that enables a continuous variable opening degree. The system has temperature and pressure sensors on each side of the components in the refrigeration cycle. Mass flow meters measures the mass flow rates of refrigerant in the refrigeration cycle and water on the secondary side of the evaporator. Temperature sensors measure the inlet and outlet temperature of the secondary media on respectively the evaporator and the condenser. The applied power to the condenser fan and the compressor is measured. Finally the entire test system is located in a climate controlled room, such that the ambient temperature can be regulated. For data acquisition and control the XPC toolbox for SIMULINK is used.

III. Modeling and verification

A. Model overview

A detailed model for an evaporator based on the conservation equations of mass, momentum and energy on the refrigerant, air and tube wall. This leads to a numerical solution of a set of differential equations discretized into a finite difference form, see [5]. This model gives very detailed information to the control designer comparable to the real system. This means that it is useful for testing of controllers, but due to the high complexity not for design of new control principles.

A simpler model may be obtained by using a so called moving boundary model for the time dependent two phase flows and by assuming that spatial variations in pressure are negligible, wich means that the momentum equation is no longer necessary. The numerical solution may describe the system quite well and results are shown in [2] and [3]. The moving boundary model is very general and may be fitted to most evaporator types.

By simplifing of the moving boundary model further a very simple nonlinear model describing the dominating time "constant" and the nonlinear behavior between input and output is obtained. The gain and time constant variations as a function of the inputs and disturbances are expressed analytically. Following approximations made are

- fluid flow is one-dimensional
- spatial variations in pressure are negligible
- axial conduction is negligible
- cross sectional area of flow stream is constant
- the heat transfer coefficient from water to wall is small compared to the heat transfer coefficient from wall to boiling refrigerant
- the energy for super heating the gas is negligible compared to the energy for evaporating the refrigerant
- the heat capacity of the wall between water and refrigerant is considered to be negligible.

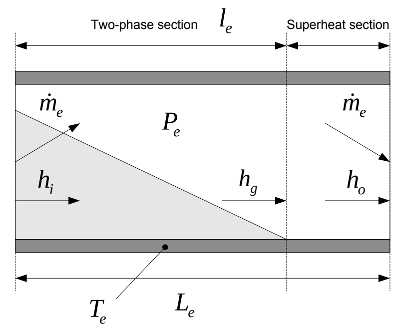

Fig. 2. Schematic drawing of the evaporator

B. Energy and mass balance two phase section

The mass and energy of the two phase section are given by

$$\begin{aligned} M_e(t) &= (\rho_l(1-\gamma_e)+\rho_g\gamma_e)BHl_e(t) \\ U_e(t) &= (\rho_l(1-\gamma_e)h_l+\rho_g\gamma_e h_g)BHl_e(t) \end{aligned} \tag{1}$$

where it is assumed that the work associated with the rate of change of pressure with respect to time is negligible. From (1) the following relation is obtained

$$U_e - h_g M_e = -\rho_l(1-\gamma_e)(h_g-h_l)BHl_e \tag{2}$$

If it is furtherly assumed that void fraction γ_e is constant independent of l_e, and variation of h_g and h_l due to pressure variation is neglected, the following relation is obtained

$$\dot{U}_e - h_g\dot{M}_e = -\rho_l(1-\gamma_e)(h_g-h_l)BH\frac{dl_e}{dt} \tag{3}$$

The mass and energy balance is given by

$$\begin{aligned} \dot{M}_e &= \dot{m}_e - \dot{m}_{comp} \\ \dot{U}_e &= h_i\dot{m}_e - h_g\dot{m}_{comp} + \alpha_1 Bl_e(T_{water}-T_e) \end{aligned} \tag{4}$$

Combining (3) and (4) then gives

$$\begin{aligned} &\rho_l(1-\gamma_e)(h_g-h_l)BH\tfrac{dl_e}{dt} = \\ &(h_g-h_i)\dot{m}_e - \alpha_1 Bl_e(T_{water}-T_e) \end{aligned} \tag{5}$$

The first term on the right side corresponds to the energy difference between the refrigerant leaving and entering the two phase section of the evaporator. The second term is the rate of the heat transfer from water to refrigerant. The left side describes the change of energy of the two phase section. From refrigerant data [10] we have

$$\begin{aligned} h_g &= HDewP(P_e) \\ h_i &= HBubP(P_c) \\ h_l &= HBubP(P_e) \\ T_e &= TDewP(P_e) \\ \rho_g^{-1} &= VDewP(P_e) \\ \rho_l^{-1} &= VBubP(P_e) \end{aligned} \tag{6}$$

Insertion of (1) in (4) then gives

$$\frac{d(\rho_l(1-\gamma_e)+\rho_g\gamma_e)BHl_e}{dP_e}\frac{dP_e}{dt} = \dot{m}_e - \dot{m}_{comp} \tag{7}$$

Assuming the liquid to be incompressible (7) becomes

$$BHl_e\kappa\frac{dP_e}{dt} = \dot{m}_e - \dot{m}_{comp} \tag{8}$$

with $\kappa = \frac{d\rho_g}{dP_e}$.

C. Superheat section

If the axial conduction is negligible and the heat capacity of the water $c_p\dot{m}_{water} >> c_{p,e}\dot{m}_e$ the superheat T_{SH} becomes

$$T_{SH} = (T_{water} - T_e)\left[1 - \exp\left\{-\frac{\alpha_1 B(L_e - l_e))}{c_{p,e}\dot{m}_e}\right\}\right] \quad (9)$$

D. Compressor

The piston compressor model is developed from factory given data as

$$\dot{m}_{comp} = \alpha_c P_e f_c \quad (10)$$

where α_c is a function of P_e and P_c. Assuming $P_c = P_{c,ref}$ due to control of the condenser fan the variation of α_c is only caused by variation of P_e. In the working area for the system this variation is less than 5% and α_c is considered as a constant. Equ. (10) in (8) then gives

$$\frac{BHl_e\kappa}{\alpha_c f_c}\frac{dP_e}{dt} = -P_e + \frac{\dot{m}_e}{\alpha_c f_c} \quad (11)$$

E. Combined model

$$\begin{aligned} T_e &= TDewP(P_e) \\ c_1\dot{x}_e &= (h_g - h_i)\dot{m}_e - c_0(T_w - T_e)x_e \\ c_2\frac{f_{\min}}{f_c}\dot{P}_e &= -P_e + \frac{\dot{m}_e}{\alpha_c f_c} \\ T_{SH} &= (T_w - T_e)\left[1 - \exp\left\{-\frac{1-x_e}{x_\delta}\right\}\right] \end{aligned} \quad (12)$$

with:

a) $c_1 = \rho_l(1-\gamma_e)(h_g - h_l)BH$
b) $c_2 = BHl_e\kappa/(\alpha_c f_{\min})$
b) $c_0 = \alpha_1 BL_e$
c) $x_\delta = c_{p,e}\dot{m}_e/(\alpha_1 BL_e)$
d) $x_e = l_e/L_e$

F. Control input and measurement

The control inputs are f_c and $\dot{m}_e$ and the measured values are T_{SH}, P_e and T_w. From these measurements the relative length x_e of the two phase section is obtained by

$$x_{e,meass} = 1 - x_\delta \log\frac{T_w - T_e}{T_w - T_e - T_{SH}} \quad (13)$$

G. Model verification

The model parameters to be estimated are (c_1, c_2) and $\theta = (\alpha_c, x_\delta, c_0)$. A series of experiments giving large signal excitation of the system for different working conditions are performed. Simulation using the model (12) with the same input $(\dot{m}_\nu, f_{comp,ref})$ as used in the experiment then gives the output (P_e, T_{SH}). The constants c_1 and c_2 are first found by visual fitting of simulated and measured values of the output. Using these values for all experiments θ may now be determined by minimizing the performance function

$$J(\theta) = \frac{1}{t_2 - t_1}\int_{t_1}^{t_2}\{K_0(P_e - P_{e,meass})^2 + (T_{SH} - T_{SH,meass})^2\}dt \quad (14)$$

where $K_0 = 50$ gives a reasonable weight between variation of P_e and T_{SH}. The result is shown in table I

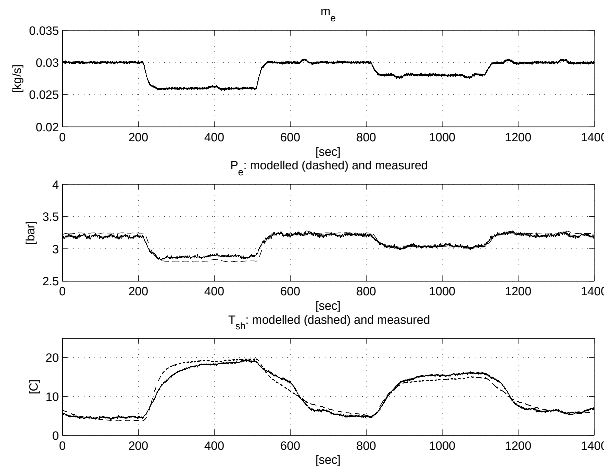

Fig. 3. Modeled (dashed) and measured P_e and T_{sh} for variation of input $\dot{m}_e$

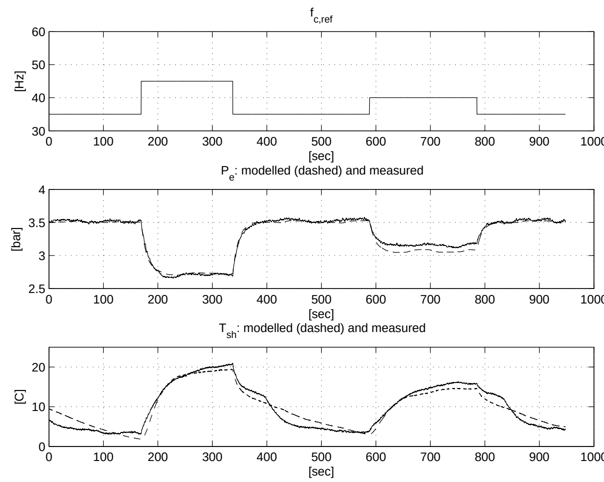

Fig. 4. Modeled (dashed) and measured P_e and T_{sh} for variation of input $f_{c,ref}$

Simulated and measured values for experiment 2 and 4 are shown in fig. (3) and (4). It is seen that the model gives a good description of the dominating dynamics of the system when optimized values are used. Fig. (5) shows the simulated output using the estimated mean values. The dynamics are again well described but DC values are badly modelled. This means that the DC value problem needs a special treatment.

IV. New control methods

The steady state value of the pressure given by the model

$$c_2\frac{f_{\min}}{f_c}\dot{P}_e = -P_e + \frac{\dot{m}_e}{\alpha_c f_{c,ref}} \quad (15)$$

is proportional to $\dot{m}_e/\alpha_c$. In the model verification section the uncertenty of α_c was shown. The refrigerant flow $\dot{m}_e$ was measured, but in a practical control scheme an estimate of $\dot{m}_e$ has to be used. This means that the gain $\dot{m}_e/\alpha_c$ may have an error up to 30% of the best guess. Because the measured

TABLE I

EXPERIMENTS FOR MODEL VERIFICATION

	Experiment		c_1	c_2	α_c	x_δ	c_0	J
1.	$f_{c,ref} = 40$	and $0.020 < \dot{m}_e < 0.024$	$3e5$	10	$1.7757e-4$	0.1604	242.6	1.4373
2.	$f_{c,ref} = 50$	and $0.026 < \dot{m}_e < 0.030$	$3e5$	10	$1.8682e-4$	0.1310	274.5	1.2464
3.	$f_{c,ref} = 60$	and $0.029 < \dot{m}_e < 0.033$	$3e5$	10	$1.8015e-4$	0.1957	294.5	3.2409
4.	$\dot{m}_e = 0.022$	and $35 < f_{c,ref} < 45$	$3e5$	10	$1.7925e-4$	0.1429	223.7	2.3106
5.	$\dot{m}_e = 0.028$	and $45 < f_{c,ref} < 55$	$3e5$	10	$1.8282e-4$	0.1390	265.2	3.5094
6.	random		$3e5$	10	$1.7765e-4$	0.1650	238.9	1.9463
7.	random		$3e5$	10	$1.8673e-4$	0.1494	269.6	1.6897
8.	random		$3e5$	10	$1.7876e-4$	0.1658	276.1	1.1648
	mean values		$3e5$	10	$1.8122e-4$	0.1562	260.6	

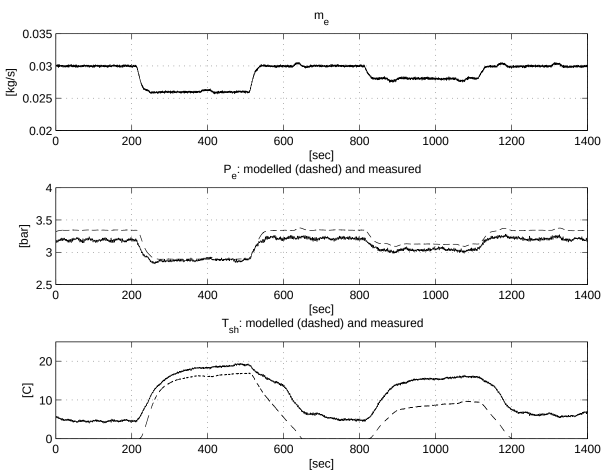

Fig. 5. Modeled (dashed) and measured P_e and T_{sh} for variation of input $\dot{m}_e$ using estimated mean values

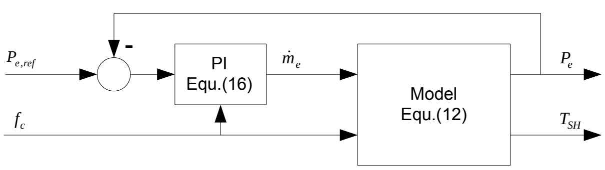

Fig. 6. Model with PI control of input m_e.

pressure P_e is of good quality a way to overcome this problem is to control the pressure by an PI-controller. The controller

$$\dot{m}_e = \frac{\alpha_c f_{c,ref}}{\tau_0} \frac{1 + c_2 \frac{f_{\min}}{f_c} p}{p} (P_{e,ref} - P_e) \tag{16}$$

gives the closed loop for the pressure

$$\tau_0 \dot{P}_e = -P_e + P_{e,ref} \tag{17}$$

The variation in the gain $\dot{m}_e/\alpha_1$ then only influence the time constant τ_0. The evaporation temperature T_e based on the pressure P_e may be calculated by

$$T_e = TDewP(P_e) \approx -a_0 + a_1 P_e \tag{18}$$

where the linear approximation is valid over a wide range. The resulting cascaded structure shown in fig. (6) thin gives the following model for the relative filling x_e and the evaporation temperature

$$\begin{aligned} c_1 \dot{x}_e &= (h_g - h_i)\alpha_c f_{c,ref} P_e - c_0 x_e (T_w + a_0 - a_1 P_e) \\ \tau_0 \dot{P}_e &= -P_e + P_{e,ref} \end{aligned} \tag{19}$$

In equation (19) x_e has to be controlled to a value x_e^0 by $P_{e,ref}$. If P_e was the control input it should be given the value P_e^0 calculated by equ. (20)

$$(h_g - h_i)\alpha_c f_{c,ref} P_e^0 - c_0 x_e (T_w + a_0 - a_1 P_e^0) = -k_1 (x_e - x_e^0) \tag{20}$$

This gives for constant x_e^0

$$\begin{aligned} c_1 p(x_e - x_e^0) &= -k_1 (x_e - x_e^0) \\ &\quad + \left((h_g - h_i)\alpha_c f_{c,ref} + c_0 x_e a_1\right)(P_e - P_e^0) \\ \tau_0 p(P_e - P_e^0) &= -(P_e - P_e^0) + P_{e,ref} - P_e^0 - \tau_0 p P_e^0 \end{aligned} \tag{21}$$

The positive definite Lyapunov function candidate

$$P = \tfrac{1}{2} c_1 (x_e - x_e^0)^2 + \tfrac{1}{2} \tau_0 k_2 (P_e - P_e^0)^2 \tag{22}$$

then has the time derivative

$$\begin{aligned} \dot{P} = &\ -k_1 (x_e - x_e^0)^2 - k_2 (P_e - P_e^0)^2 \\ &\ +(P_e - P_e^0) k_2 U \\ U = &\ P_{e,ref} - (1 + \tau_0 p) P_e^0 \\ &\ + \frac{(h_g - h_i)\alpha_c f_{c,ref} + c_0 x_e a_1}{k_2} (x_e - x_e^0) \end{aligned} \tag{23}$$

For a control input P_{ref}

$$P_{ref} = (1 + \tau_0 p) P_e^0 - \frac{(h_g - h_i)\alpha_c f_{c,ref} + c_0 x_e a_1}{k_2} (x_e - x_e^0) \tag{24}$$

giving $U = 0$ the time derivative of the Lyapunov function becomes

$$\dot{P} = -k_1 (x_e - x_e^0)^2 - k_2 (P_e - P_e^0)^2 \tag{25}$$

This function is negative definite for positive $k_1 > 0$ and $k_2 > 0$, leading to a stable closed loop system.

The new backstepping controller

$$\begin{aligned} P_e^0 &= \frac{c_0 x_e (T_w + a_0) - k_1 (x_e - x_e^0)}{(h_g - h_i)\alpha_c f_{c,ref} + c_0 x_e a_1} \\ P_{e,ref} &= (1 + \tau_0 p) P_e^0 - \frac{(h_g - h_i)\alpha_c f_{c,ref} + c_0 x_e a_1}{k_2} (x_e - x_e^0) \\ \dot{m}_e &= \frac{\alpha_c f_{c,ref}}{\tau_0} \frac{1 + c_2 \frac{f_{\min}}{f_c} p}{p} (P_{e,ref} - P_e) \\ \dot{m}_e &= sat(\dot{m}_e, \dot{m}_{e\,\min}, \dot{m}_{e\,\max}) \end{aligned} \tag{26}$$

The developed backstepping controller equ. (26) is tested on a simulation model based on estimated mean value model

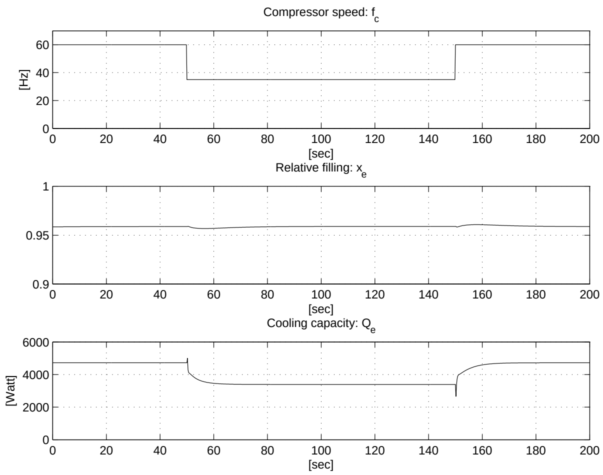

Fig. 7. simulated x_e and P_e for variation of input m_ν using the backstepping controller for known parameters

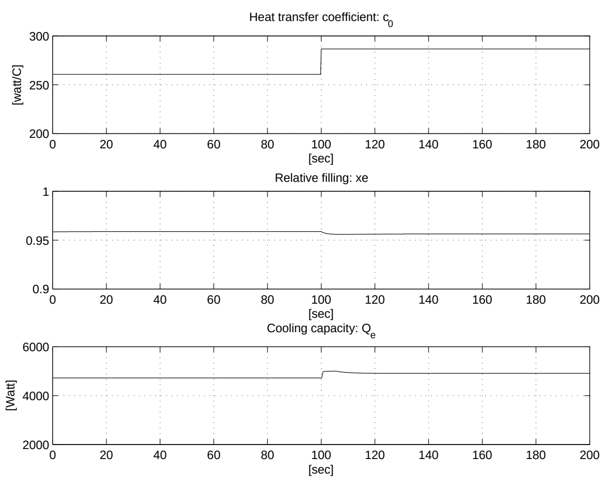

Fig. 8. simulated x_e and P_e for variation of c_0 using the backstepping controller for constant c_0 equal to the value before the change.

parameters. The result is shown in fig. 7 for the following controller parameters

$$
\begin{aligned}
\tau_0 &= 2 \\
k_1 &= 10^6 \\
k_2 &= 10^6 \\
x_e^0 &= 0.96 \\
a_0 &= 26 \\
a_1 &= 8.5
\end{aligned} \tag{27}
$$

based on model knowledge. The variation in x_e caused by the variation in m_e is small due to the small time constant τ_0 for the pressure controller. In the controller c_0 is assumed known leading to a steady state m_e equal to the reference.

Fig. 8 shows the simulated output if c_0 is changed during the simulation. The figure shows no the need for an adaptation of the c_0 value.

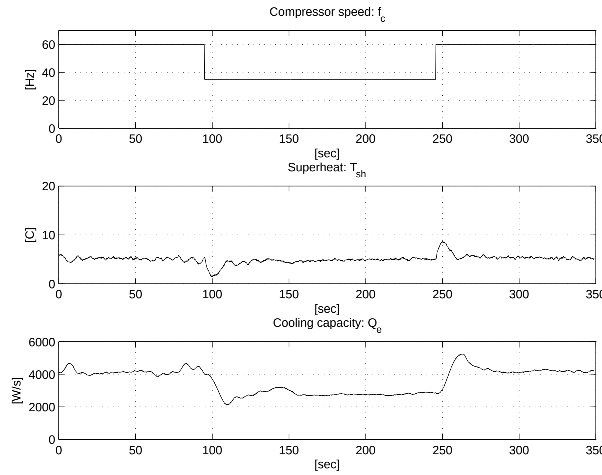

Fig. 9. Measured f_c, T_{sh} and $\dot{Q}_e$ using the backstepping controller

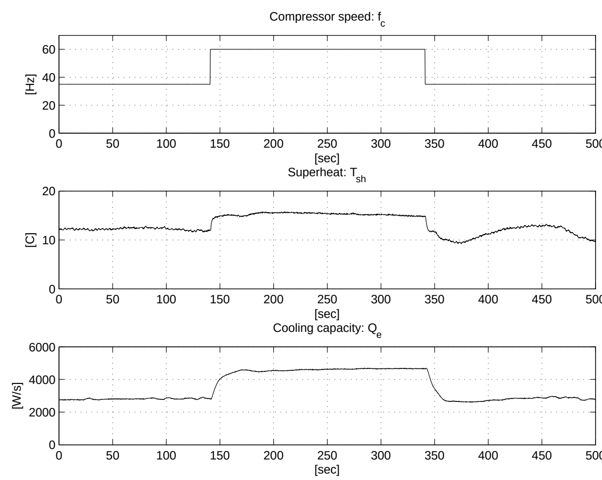

Fig. 10. Measured f_c, T_{sh} and $\dot{Q}_e$ using a conventional TXV controller

V. Experiments

Fig. 9 shows the performance of the new controller for a step change of the compressor speed f_c between maximum and minimum. Only a small variation of the superheat temperature is seen even if the superheat reference is as low as 5 degree Celsius. The figure also shows the variation of the cooling capacity. Fig. 10 shows the same experiment for a conventional TXV controller. The disturbance of the superheat temperature due to step in compressor speed is significant compared to fig. 9 and may lead to hunting effects. Fig. 11 shows the startup of both the new controller and the TXV controller. The lower curve in the figure is the new controller and it is seen to obtain the steady state value faster than the TXV controller. This means that pulse width modulation during low load may be more energy efficient with the new controller.

VI. Conclusion

A new control strategy is compared to a conventional control strategy based on a thermostatic expansion valve for control of the superheat. A low order model for the highly nonlinear

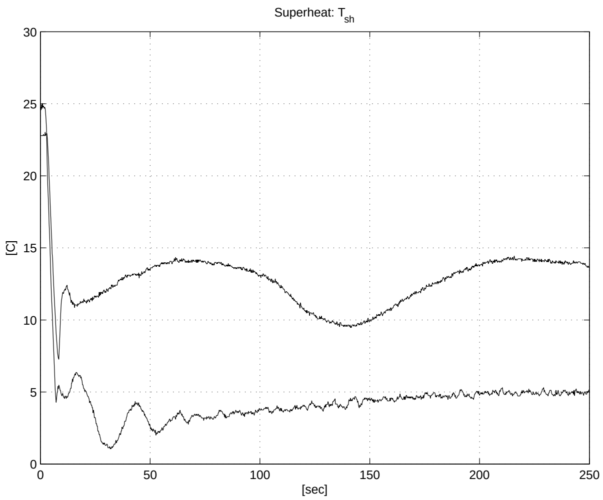

Fig. 11. Measured T_{sh} at startup. The lower curve is the new controller and the upper curve is the conventional TXV controller.

system with compressor speed and refrigerant flow as inputs and superheat as output is derived and verified experimentally. The model has a form where backstepping may be used as a nonlinear design method. The developed method gives a superheat control which is nearly independent of the cooling capacity. The stability of the proposed method is validated theoretically by Lyapunov analysis and experimental results shows the performance of the system for a wide range of operating points.

Compared to other methods no gain scheduling of the superheat controller is necessary to cover a large region of operation. The comparison between this new controller and the conventional TXV controller shows that continuous control is possible for all values of the cooling capacity with the new controller.

REFERENCES

[1] Aaström, K.J. and B. Wittenmark. *Adaptive Control - Second Edition*, Addison-Wesley, 1995.

[2] Grald, E.W. and J.W. MacArthur (1992). Moving boundary formulation for modeling time-dependent two-phase flows. *Int. J. heat and Fluid Flow* **13**, 266–272.

[3] He, X.D., H.H. Asada, S. Liu and H. Itoh (1998*a*). Multivariable control of vapor compression systems. *HVAC&R Research* **4**, 205–230.

[4] He, Xiang-Dong, Sheng Liu, Harry H. Assada and Hiroyuki Itoh (1998*b*). Multivariable control of vapor compression system. *VAC&R Research*.

[5] Jia, X., C.P. Tso, P. Jolly and Y.W. Wong (1999). Distributed steady and dynamic modeling of dry-expansion evaporators. *Int. Journal of Refrigeration* **22**, 126–136.

[6] Lei, Zhao and M. Zaheeruddin (2005). Dynamic simulation and analysis of water chiller refrigeration system. *Applied Thermal Engineering* **25**, 2258–2271.

[7] Parkum, J. and C. Wagner (1994). Identification and control of a dry-expansion evaporator. *10th IFAC symposium on system identification*.

[8] Larsen, L.F.S (2005). Model Based Control of Refrigeration Systems. *Ph.D. Thesis ISBN 87-90664-29-9*. Aalborg University / Danfoss A/S.

[9] Larsen, L.F.S. and C. Thybo (2004). Potential energy savings in refrigeration systems using optimal setpoints. *Conference on Control Applications*, Taipei, Taiwan.

[10] Skovrup M. J. Thermodynamic and Thermophysical Properties of Refrigerants. Ver. 3.00, 2000, Technical University of Denmark.

[11] Changquin Tian, Chunpeng Dou, Xinjiang Yang and Xianting Li. Instability of automotive air conditioning system with a variable displacement compressor. Part 1. Experimental investigation, *International Journal of Refrigeration*, no28, 2005.